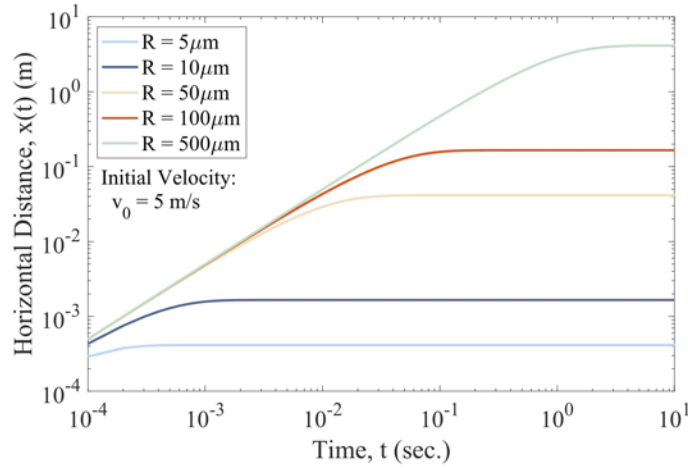


Supplementary Materials:

1. Stopping distance of Droplets

The horizontal movement, $x(t)$, of droplets is well known and described by Eq. 1, where v_0 is the initial horizontal velocity of the particle, η is the dynamic viscosity of the air, and ρ_d and R are the density and radius of the droplet. As shown in Supplementary Figure 1, for a single droplet with diameter $R = 10$ micron and, initial velocity $v_0 = 5$ m/s, a maximum horizontal travel distance (also called the stopping distance) of ~ 1 mm is obtained, whereas a droplet with radius 100 micron at the same initial velocity will have a stopping distance of about 10cm.

$x(t) = \frac{2v_0(\rho_d - \rho_a)R^2}{9\eta} \left(1 - e^{-\frac{9\eta t}{2(\rho_d - \rho_a)R^2}}\right)$	Eq. 1
---	--------------

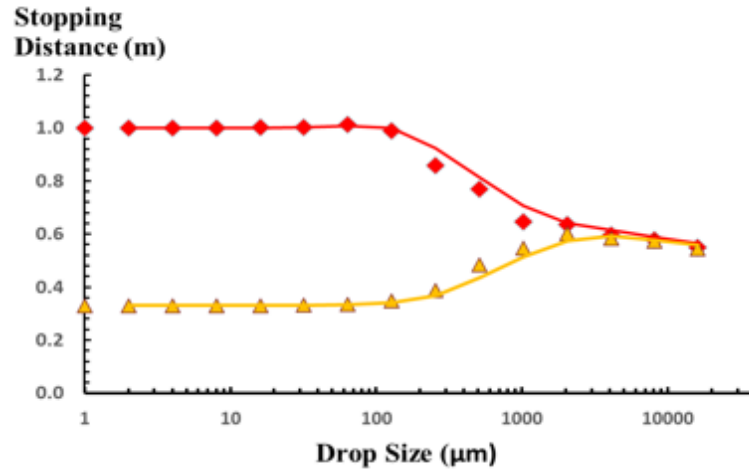


Supplementary Figure 1 – Temporal evolution of horizontal travel distances for a broad range of droplet sizes.

The horizontal movement of the micro-droplets is not only influenced by their own initial velocity, but also by the movement of bulk air displaced by coughing or speaking. Using a Stokes flow approximation, the influence of how the air stream with initial velocity v_0 ‘carries’ these droplets can be determined. Eq. 2 gives the horizontal travel distance of the droplets in the air stream where $r \equiv \sqrt{9\eta/2\lambda\rho}$ and λ sets the maximum stopping distance of the air stream which may be obtained experimentally.

Supplementary Figure 2 shows that the micro-droplets are predicted to travel 1m in distance given an initial velocity of 1m/s.

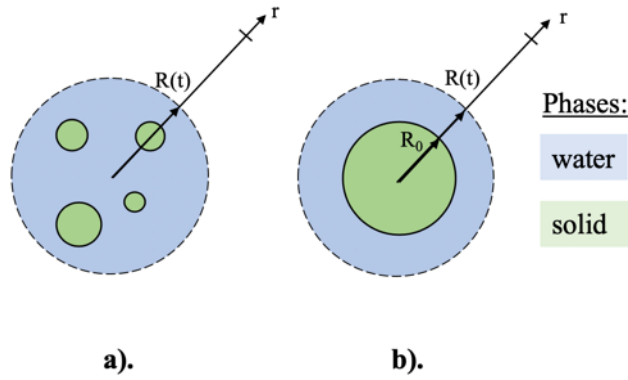
$x(t) = \frac{v_o \left(\left(\frac{R}{r} \right)^2 + 1 \right)}{\lambda} \left(1 - e^{-\lambda t / \left(\left(\frac{R}{r} \right)^2 + 1 \right)} \right)$	Eq. 2
--	--------------



Supplementary Figure 2 - Maximum travel distance as a function of droplet size for droplets emitted inside a cough having a stopping distance of 0.33 m (yellow) and another one having a stopping distance of 1.0 m (red), both released at 1.5 m above the floor with initial velocities of 0.3m/s and 1 m/s, respectively.

2. Evaporation of Droplets

The evaporation of a spherical droplet in an environment with a known relative humidity (RH), idealized in Supplementary Figure 3a/b, can be evaluated using the diffusion model presented and validated in [8,9]. The rate of change of the mass of the droplet, $m_d(t)$, is given by Equation 3, where $R(t)$ is the radius of the droplet, D_{va} is the diffusivity of water vapor in air, and $C(r,t)$ is the water vapor concentration along direction r . Assuming that the droplets are sufficiently spaced and that the relative humidity of the air in which they are falling through does not change, Equation 4 expresses the water vapor concentration gradient found in Eq. 3. The water vapor concentrations at the surface of droplet (i.e., $r = R(t)$) is given by the equilibrium vapor pressure, ρ_{vap} , of the environment and very far away from the droplet surface (i.e., $r \gg R(t)$) is given by the product of the RH of the environment and ρ_{vap} , resulting in Eq. 5.



Supplementary Figure 3 – a). idealized spherical droplet and b). solid core simplification.

$\frac{\partial m_d(t)}{\partial t} = 4\pi R^2(t) D_{va} \left. \frac{\partial C(r, t)}{\partial r} \right _{r=R(t)}$	Eq. 3
---	--------------

$\left. \frac{\partial C(r, t)}{\partial r} \right _{r=R(t)} = (C(r = \infty) - C(R(t), t)) \left(\frac{1}{R(t)} + \frac{1}{\sqrt{\pi D t}} \right)$	Eq. 4
---	--------------

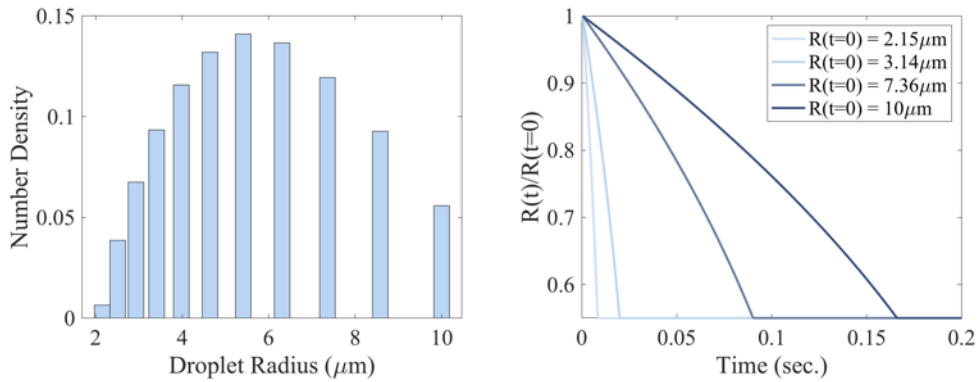
$\frac{\partial m_d(t)}{\partial t} = 4\pi R^2(t) D_{va} \rho_{vap} (RH - 1) \left(\frac{1}{R(t)} + \frac{1}{\sqrt{\pi D t}} \right)$	Eq. 5
--	--------------

The preceding equations express how the liquid water mass in the droplet reduces due to evaporation. Assuming that the solids constitute a ‘spherical core’ of the droplet, as shown in Supplementary Figure 3a, the mass, m_d , of the droplet at any time is given by Eq. 6 where ρ_s is the density of solid found in human mucus/saliva (i.e., 1500 kg/m³) from [10] and ρ_w is the density of liquid water. Differentiating Eq. 6 with respect to time and combining the result with Eq. 5 gives Eq. 7 - a non-separable differential equation for the evolution in size of the droplet due to evaporation, where evaporation stops when the droplet is completely composed of the solid fraction or when $R(t) = R_0$. The evolving density of the droplet, $\rho_d(t)$, is obtained by Eq. 8. For the purpose of the following calculations, it is taken that the R_0 for each droplet is a factor of two of $R(t=0)$ and corresponds to an initial density of ~ 1080 kg/m³ for water – solid droplet mixture. Supplemental Figures 4 and 5 display solutions to Eq. 7 for numerous micro-droplet sizes and the influence of the RH on the evaporation kinetics of a 10 micron droplet. Within 1 second, the evaporation of the small micro-droplets is complete, resulting in a solid-core laden with virus copies.

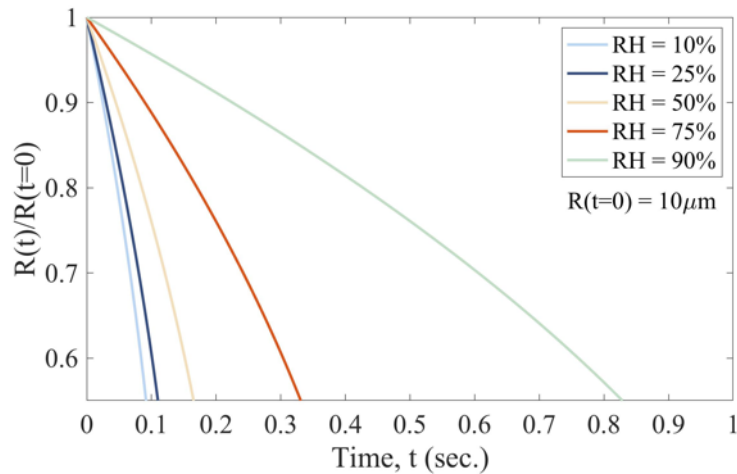
$m_d(t) = \frac{4\pi}{3} R_0^3 \rho_s + \frac{4\pi}{3} (R^3(t) - R_0^3) \rho_w$	Eq. 6
---	--------------

$\frac{\partial R(t)}{\partial t} = \frac{\rho_{vap} D_{va}}{\rho_w} (RH - 1) \left(\frac{1}{R(t)} + \frac{1}{\sqrt{\pi D_{va} t}} \right)$	Eq. 7
--	--------------

$\rho_d(t) = \frac{3m_d(t)}{4\pi R^3(t)}$	Eq. 8
---	--------------



Supplementary Figure 4 – a). initial size distribution of microdroplets generated by human speech, b). normalized size evolution due to evaporation for each size class given in a). in an environment with RH = 50%.



Supplementary Figure 5 – Influence of relative humidity on the evaporation kinetics of a $R(t=0) = 10$ micron droplet.

3. Sedimentation and Persistence of Droplets

At all times, the droplets are assumed to be vertically falling at their terminal velocities described by Stokes flow. Eq. 9 describes the rate of change of the height, $h(R(t),t)$, through which the droplet has fallen where ρ_a is the density of air and g is the acceleration due to gravity. By solving Eq. 7 and Eq. 9 numerically, the progressive evaporation and sedimentation of the droplets is coupled and comparable to models presented in [11,12]. For the framework presented herein, how the number of droplets in a given volume evolve can be predicted, allowing for the persistence calculations in Figure 3 to be made. For this calculation, it is assumed that the droplets of each size class have a uniform random initial height in the volume in which they progressively sediment. From the particle size distribution, the total number of particles of each size class, $N(R(t=0))$, initially in the volume can be obtained. The evolution in the total number of particles for each size class is then directly given by Eq. 10 while $h(R(t),t)$ is less than the system height, h_{sys} . The total number of droplets in the system, N_{total} , at any time, t , is then the discrete summation of Eq. 10 over all particle sizes, n , for which $h(R(t),t) < h_{sys}$ shown in Eq. 11.

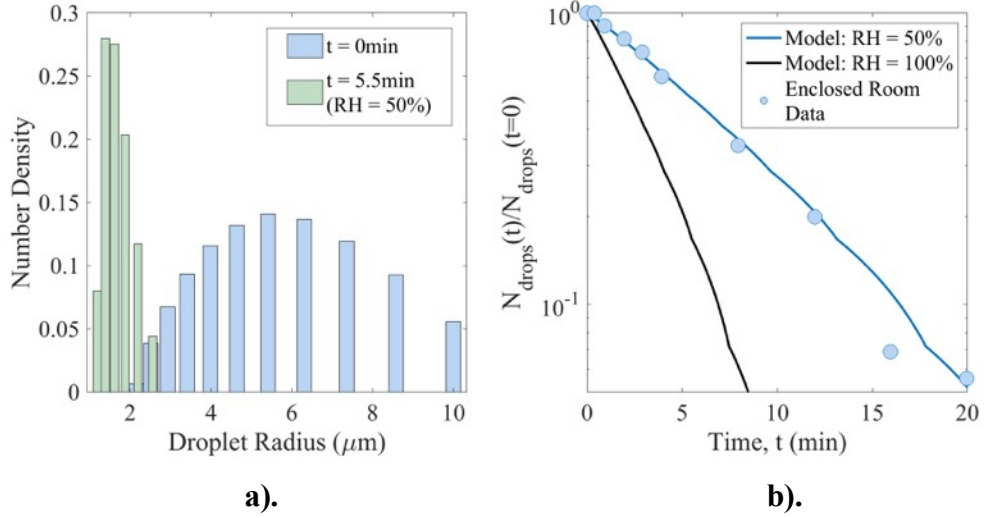
$\frac{\partial h(R(t), t)}{\partial t} = \frac{2(\rho_d(t) - \rho_a)}{9\eta} gR^2(t)$	Eq. 9
--	--------------

$N(R(t), t) = N(R(t = 0)) \frac{h(R(t), t)}{h_{sys}}$	Eq. 10
---	---------------

$N_{total}(t) = \sum_{i=1}^n N(R(t), t)$	Eq. 11
--	---------------

Figure 3 displays that the derived system of equations and model system can directly predict the persistence of the aerosol particles with knowledge of the system size, initial size distribution of the aerosol droplets, and the relative humidity. Supplementary Figure 6a displays how the droplet size distribution evolves due to effects of evaporation and sedimentation at 5.5min, which corresponds to when ~50% of the initial number aerosol particles (i.e., the halflife) remain in the space. Supplementary Figure 6b, shows that the halflife reduces nearly 50% when the relative humidity is 100% - corresponding to conditions in which there is no evaporation of the aerosol. As expected, when no evaporation occurs, the droplets fall faster through the system due to their nominally larger size and higher terminal velocities. The decrease in number of

microdroplets in the system due the effects of higher relative humidity implies a lower-likelihood of aerosol mediated transmission of CoV-2, as presented in Figure 4, and corresponds to other studies [13,14] that show that higher relative, and absolute, humidity environments may lead to lower infectivity rates of influenza and other respiratory infections.



Supplementary Figure 6 – a). change in droplet size distribution due to sedimentation and evaporation at the half-life of droplet evolution, **b).** influence of relative humidity on droplet evolution.

4. A General Persistence Model

Based on these results, a more general model can be derived to explain the exponential decline in droplets. Given a number N_0 of drops with a given diameter D , then it is reasonable to assume that the decrease in time will be exponential and given by

$N(D, t) = N_0 e^{-\alpha D^2 t}$	Eq. 12
-----------------------------------	---------------

with α an empirical constant independent of the droplet diameter D . A good estimate of $\alpha \cong \rho g / 18 \eta h$ with h a typical sedimentation height. The life time of a micro-droplet is then characterized by the exponent in Eq. 12, and given by $t_{\text{life}} \equiv 1 / \alpha D^2$.

In case of droplets with a varying size distribution we have to collect the different droplet sizes and get:

$$N_{total}(D, t) = \sum_{i=1}^{i=n} N_i e^{-\alpha D^2 t}$$

Eq. 13

Supplementary Material References:

8). P.S. Epstein, M.S. Plesset, On the stability of gas bubbles in liquid-gas solutions, Chem. Phys. 18 (1950) 1505-1509.

9). P.B. Duncan, D. Needham, Test of the Epstein-Plesset Model for gas microparticle dissolution in aqueous media: effect of surface tension and gas undersaturation in solution, Langmuir 20 (2004) 2567-2578.

10). 3). K.R. Bhaskar, D.D. O'Sullivan, J. Seltzer, T.H. Rossing, J.M. Drazen, L.M. Reid, Density gradient study of bronchial mucus aspirates from healthy volunteers (smokes and nonsmokers) and from patients with tracheostomy, Exp Lung Res (1985) 9 289-308.

11). X. Xie, Y. Li, A.T.Y. Chwang, P.L. Ho, W.h. Seto, How far droplets can move in indoor environments – revisiting the Wells evaporation-falling curve, Indoor Air (2007) 17:211-225, DOI: 10.1111/j.1600-2006.00469.x

12) Redrow J, Mao S, Celik I et al. Modeling the evaporation and dispersion of airborne sputum droplets expelled from a human cough. *Build Environ.* 2011; **46**: 2042–2051.

13). Noti JD, Blachere FM, McMillen CM, Lindsley WG, Kashon ML, Slaughter DR, et al. (2013) High Humidity Leads to Loss of Infectious Influenza Virus from Simulated Coughs. PLoS ONE 8(2): e57485. <https://doi.org/10.1371/journal.pone.0057485>

14). J. Shaman, M. Kohn, Absolute humidity modulates influenza survival, transmission, and seasonality, PNAS (2009) 109 (9) 3243 – 3248, <https://doi.org/10.1073/pnas.0806852106>